CIMAC CONGRESS 25
ZURICH, MAY 19 – 23, 2025

2025 | 501

Ammonia pre-chamber engine combustion with online ammonia cracking

Visualizations

Jiuling Sun, Tianjin University

Qinglong Tang, Tianjin University
Xuze Zhu, Tianjin University
Mingsheng Wen, Tianjin University
Linhui Huang, Tianjin University
Zhenyang Ming, Tianjin University
Haifeng Liu, Tianjin University
Mingfa Yao, Tianjin University

This paper has been presented and published at the 31st CIMAC World Congress 2025 in Zürich, Switzerland. The CIMAC Congress is held every three years, each time in a different member country. The Congress program centres around the presentation of Technical Papers on engine research and development, application engineering on the original equipment side and engine operation and maintenance on the end-user side. The themes of the 2025 event included Digitalization & Connectivity for different applications, System Integration & Hybridization, Electrification & Fuel Cells Development, Emission Reduction Technologies, Conventional and New Fuels, Dual Fuel Engines, Lubricants, Product Development of Gas and Diesel Engines, Components & Tribology, Turbochargers, Controls & Automation, Engine Thermondynamis, Simulation Technologies as well as Basic Research & Advanced Engineering. The copyright of this paper is with CIMAC. For further information please visit https://www.cimac.com.

ABSTRACT

Ammonia is regarded as a highly promising alternative fuel in the transportation sector due to its carbon-free nature. However, ammonia combustion has the disadvantage of poor flammability and combustion sluggishness. It is necessary to employ advanced combustion technologies to improve its combustion performance Pre-chamber ignition (PCI) technology can generate multiple distributed ignition sites and significantly improve combustion stability and flame propagation speed. Hydrogen addition can enhance the activity of the fuel mixture. Both methods can improve the combustion performance of ammonia. A narrow-throat passive pre-chamber (PC) was designed in this study. Hydrogen production by ammonia cracking was applied to investigate the effect of partial ammonia cracking on combustion performance under the pre-chamber ignition mode and spark ignition (SI) modes. The findings reveal that increasing the ammonia cracking ratio effectively improves the combustion performance in both ignition modes. The combustion performance in the PCI mode is inferior to that of the SI mode due to the heat transfer loss in the pre-chamber under pure ammonia combustion conditions. When the ammonia cracking ratio increases from 0 to 10%, the combustion performance is significantly improved in the PCI mode, while the improvement is relatively small in the SI mode. The hydrogen addition through ammonia cracking is a feasible pathway to achieve stable combustion and high-efficiency operation of the ammonia pre-chamber engine.

Keywords: Ammonia combustion; Pre-chamber ignition; Spark ignition; Partial ammonia cracking; Optical diagnostics.

1 INTRODUCTION

The energy crisis and greenhouse effect urgently require the application of clean and sustainable alternative fuels in the transportation sector. Ammonia is regarded as a highly promising alternative fuel because of its carbon-free nature and high hydrogen content by mass (17.8%) [1]. However, the widespread application of ammonia as an alternative fuel is limited by various factors, such as narrow flammability limit, slow laminar flame speed, and high minimum ignition temperature [1, 2]. The widely used method to overcome the combustion sluggishness of ammonia is the introduction of high-reactivity fuels. Commonly blending fuels in ammonia spark ignition (SI) engines consist of methane [3, 4], gasoline [5, 6], and hydrogen (H_2) [7, 8]. Notably, hydrogen addition to ammonia gained the most attention due to its carbon-free nature and high flame speed. In compression ignition (CI) engines, the widely used pilot ignition fuels are diesel [9, 10], dimethyl ether (DME) [11, 12], and n-heptane [13]. However, the high-reactivity fuel introduction requires an additional fuel supply and injection system, which increases the cost and complexity.

To maximize the carbon-free advantages of ammonia without changing the original engine structure as much as possible, the pre-chamber ignition (PCI) mode is applied to enhance the flame propagation speed of ammonia and improve engine combustion performance in this study. Pre-chamber ignition can produce multiple distributed ignition sites [14], which may overcome the poor flammability of ammonia and accelerate flame propagations. Liu et al. [15] investigated the impacts of injecting high-reactivity fuels into the pre-chamber on the performance of an all-metal ammonia PCI engine. The results show that the higher indicated mean effective pressure (IMEP) and indicated thermal efficiency (ITE) in PCI mode can be obtained than in SI mode because of the shorter ignition delay and combustion duration.

However, in previous research, the author found that pre-chamber ignition has limited effects on improving ammonia combustion performance. As mentioned earlier, hydrogen addition can effectively improve the combustion performance of ammonia, but hydrogen faces challenges in storage and transportation [16]. This paper proposes improving ammonia combustion performance through hydrogen production via ammonia decomposition. The principle of hydrogen production through ammonia decomposition is based on high-temperature catalytic cracking of ammonia, and the reaction equation is $2NH_3 \rightarrow 3H_2+N_2$ [17]. Hydrogen production by ammonia decomposition for engine operation can be divided into two categories [18]. One is in-cylinder ammonia reforming via fuel-rich combustion. Zhou et al. [19] proposed the in-cylinder reforming gas recirculation, in which one cylinder was operated at rich ammonia, and the excess ammonia was partially decomposed into hydrogen. They found it can enhance the thermal efficiency and reduce the nitrogen-based emissions. Liu et al. [20] studied hydrogen production by in-cylinder ammonia reforming from ammonia-rich combustion. The finding presents that hydrogen production increased as the initial temperature increased from 1200 K to 1300 K, and first increased then decreased with the increase of initial pressure from 22 bar to 36 bar. The other is ammonia dissociation by an on-board ammonia cracker. Klawitter et al. [17] investigated the turbulent flame propagation and combustion behaviors of pure ammonia and partially cracked ammonia under engine-like conditions. They found that the flame speed under turbulent conditions is higher than that of laminar conditions, and partial cracking of ammonia can accelerate the turbulent flame speed. Mercier et al. [21] researched the effect of cracking ratios on engine performance and emissions. The results showed that a small rate of ammonia dissociation (10%) could enhance the operating range. Wang et al. [22] applied nitric oxide laser-induced fluorescence (NO-LIF) to study the NO mole fraction in NH_3-H_2-N_2 (produced by ammonia cracking) flames. The results presented increasing the ammonia cracking ratio can reduce the NO concentration. Liu et al. [18] pointed out that a separate electrically heated hydrogen generation system independent of the engine system is more effective in producing hydrogen than thermochemical fuel reforming. Therefore, this study investigates the partial ammonia cracking based on the on-board ammonia cracker. To date, there is a lack of understanding of the pre-chamber ignition mechanism under partial ammonia cracking conditions. The pros and cons of ammonia pre-chamber ignition compared to spark ignition remain to be clarified.

In this study, we apply the natural flame luminescence (NFL) imaging technology to study the effect of ammonia cracking on combustion performance and flame development under the pre-chamber ignition (PCI) mode. Meanwhile, the combustion behaviors of ammonia-hydrogen-nitrogen mixtures between pre-chamber ignition and spark ignition (SI) are compared. This study can guide the application of ammonia as an alternative fuel in IC engines and provides an in-depth understanding of ammonia cracking effects on pre-chamber ignition engines.

2 EXPERIMENTAL SETUP

2.1 Optical engine

The experimental research was conducted on a single-cylinder optical engine. The specific parameters of the optical engine are illustrated in Table 1. The experimental setup is shown in Figure 2. The experimental setup mainly consists of four parts, i.e., optical engine, fuel supply system, data acquisition system, and monitoring and control systems.

Natural flame luminosity (NFL) imaging was applied in this study to record the combustion information of the main chamber (MC) using a high-speed camera. The lens aperture, frame rate, and spatial resolution of the high-speed camera were fixed at F1.4, 20,000 frames per second (fps), and 512 × 512 pixels, respectively. A pulse delay generator (DG645, Stanford) was employed to synchronize the trigger of ignition and high-speed camera shooting. A spark plug with an integrated pressure sensor (TI23, AVL) was utilized to ignite the fuel in the pre-chamber (PC) and collect the pressure of the PC, the main chamber pressure was collected by a pressure sensor (6125C, Kistler) mounted on the cylinder head. The pressure data were amplified by the charge amplifier (5018A, Kistler) and then transmitted to the combustion analyzer developed by our group.

Ammonia (purity is 99.9%) is stored in a 100L fuel tank at a pressure of 15 MPa, where it exists as a two-phase mixture of gas and liquid, with the gaseous ammonia generated by the vaporization of the liquid ammonia. The output pressure of the gaseous ammonia is 3 bar after pressure regulation. The ammonia line is divided into two branches. The majority of the ammonia flows directly into the surge tank, while a smaller portion goes into the NH_3 cracker and decomposes into hydrogen (H_2) and nitrogen (N_2).

Table 1 The main optical engine specifications

Parameters	Values
Engine type	4-stoke, 2-valve, water-cooled
Bore	92 mm
Stroke	100 mm
Displacement	0.664 L
Combustion chamber diameter	63 mm
Connecting rod length	155 mm

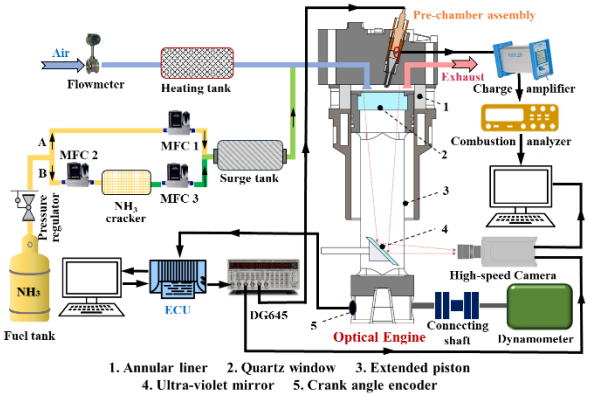

Fig. 1. The schematic diagram of the optical engine setup

The ammonia cracker (HBAQFC-5) applied in this study is produced by Hongbo Gas Equipment Technology CO., Ltd. Detailed parameters are listed in Table 2. Considering the small amount (⩽ 5 ppm) of residual ammonia after decomposition by this equipment, the products after decomposition are assumed to be only hydrogen and nitrogen. Two mass flow controllers (MFC) are installed upstream and downstream of the cracker. The upstream one regulates the ammonia flow entering the cracker to prevent excessive hydrogen content inside. The downstream one measured the flow rate of the hydrogen/nitrogen mixture entering the engine to ensure precise control of the cracking ratio.

Table 2 Detailed parameters of ammonia cracker

Parameters	Value
Max. gas production rate	5 Nm^3/h
Catalyst	Nickel catalyst
Decomposition temperature	850℃
Decomposition products	75% Hydrogen + 25% Nitrogen
Decomposition efficiency	99.9%
Residual ammonia content	≤5 ppm
Dew point	≤-60℃

2.2 Pre-chamber design

The pre-chamber is a small combustion chamber independent of MC, with flame propagation to MC through several small orifices [23]. Pre-chamber is mainly divided into passive and active pre-chamber [24]. For the passive pre-chamber, the PC fuel is supplied by the fuel from MC during the compression stroke, so the air-fuel equivalence ratio of the two chambers is consistent. The active pre-chamber needs to be equipped with an independent fuel supply and injection system to supply a fuel-rich mixture in the pre-chamber to

ignite the lean charge of MC [24, 25]. The active pre-chamber has the advantage of extending the lean limit, but it significantly increases the cost and complexity of the system. Since ammonia engines already suffer from unstable combustion and low thermal efficiency under stoichiometric combustion, active ammonia pre-chambers for lean combustion are unnecessary. Therefore, this study focuses on the combustion characteristic of passive ammonia pre-chambers.

The main structural parameters of PC are volume, orifice diameter, and orifice number [26, 27]. The volume fraction of PC was determined as 4% of the clearance volume according to the recommendations of Gussak et al. [28]. Hlaing et al. [29, 30] designed a unique narrow throat pre-chamber for methane operation. Tang et al. [31, 32] found that this chamber is more likely to form a higher-pressure difference between the main chamber and the pre-chamber, which increases the flame jet velocity and improves the combustion performance of the lean mixture in the main chamber. Therefore, the pre-chamber shape is designed as a tapering narrow throat with a throat diameter of 5 mm. The six orifices with a diameter of 2 mm are uniformly distributed along the axis with a jet cone angle of 150°. The PC structure diagram is illustrated in Fig. 2.

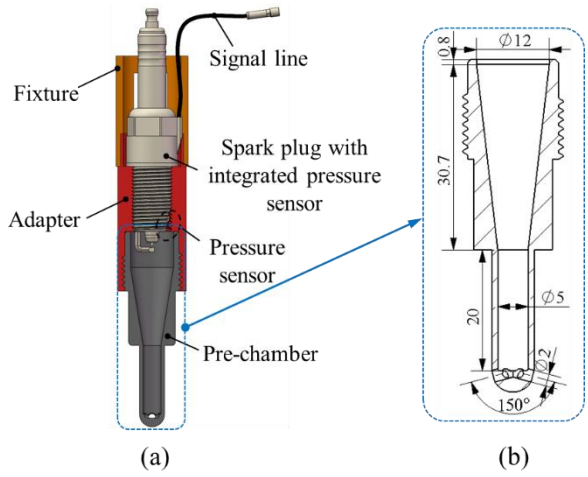

Fig. 2. Pre-chamber assembly (a) and pre-chamber geometry (b)

2.3 Operating conditions and test cases

The engine speed was maintained at 1200 revolutions per minute (rpm) by a dynamometer. The intake pressure was 1 bar and a flow meter was utilized to measure the intake air flow. The excess air ratio (λ) was fixed at 1.0 by regulating the fuel flow rate according to the detected intake airflow. The engine operating boundary conditions are shown in Table 3.

Table 3. Engine operating boundary conditions

Parameters	Value
Engine speed	1200 rpm
Coolant temperature	90℃
Excess air ratios (λ)	1.0
Intake gas	Air
Intake pressure	1 bar
Spark timings	25 °CA BTDC
Intake temperatures	25℃
Compression ratios	12.8

The degree of dissociation of NH_3 is called the cracking ratio γ, which is an important parameter for determining the hydrogen content in the fuel mixtures. The cracking ratio γ is calculated by Eq. (1) [17, 33].

$$\gamma = [NH_3]_{cracked} / [NH_3]_{init} = 2\chi_{H_2} / (3\chi_{NH_3} + 2\chi_{H_2}) \quad (1)$$

where $[NH_3]_{cracked}$ and $[NH_3]_{init}$ are the concentrations of cracked NH_3 and initial NH_3, respectively. χ is the mole fraction of different components in the fuel mixture. The investigated ammonia cracking ratios and corresponding mole fractions of the mixture components in this study are shown in Table 4, where γ=0% is the pure ammonia combustion condition. To prevent excessive hydrogen content in the mixture leading to excessive thermal load in the cylinder, which may result in damage to the engine's quartz window, the cracking ratio studied in this research is kept below 10%.

Table 4 Tested ammonia cracking ratios γ, and corresponding mole fractions χ of different components in the fuel mixture.

γ/(%)	χ_{NH_3}/(%)	χ_{H_2}/(%)	χ_{N_2}/(%)
0	100	0	0
2.5	95.1	3.7	1.2
5	90.5	7.1	2.4
7.5	86.1	10.5	3.5
10	81.8	13.6	4.6

2.4 Data processing

To quantify the flame development process, MATLAB was used to process natural flame luminosity images to extract flame propagation parameters such as flame intensity, flame area, and flame area change rate. The NFL imaging technique captures the two-dimensional projection of a three-dimensional flame. Since the combustion chamber diameter exceeds the visualization diameter of the quartz window, a mask filter was applied based on the quartz window's diameter to isolate the visual flame propagation region (inner area) from optical noise interference (outer area).

In MATLAB, the flame images were first converted into a pixel matrix. A ‘binarization-thresholding’ technique was performed to obtain a grayscale image from the RGB image, and identify the flame boundary relied on the binary result. The flame area was calculated based on the pixel count of the binarized region, which represents the projected size of the region covered by the flame during its propagation within the combustion chamber. The flame area change rate, which characterizes combustion speed, was obtained by differentiating the flame area with respect to time.

3 RESULTS AND DISCUSSIONS

3.1 Analysis of the combustion process under different ammonia cracking ratios for pre-chamber ignition

The combustion process and jet flame development of a specific cycle under different ammonia cracking ratios are shown in Fig. 3. The selected cycle has the cylinder pressure closest to the average cylinder pressure. The results indicate that the flame propagation speed in the pre-chamber is slow under the pure ammonia combustion condition shown in Figure 3 (a). The flame does not appear at the nozzle of the PC until 25 °CA after ignition, which leads to a small pressure difference of 0.8 bar under this condition. This affects the flame jet speed in the main chamber and results in a low combustion rate. Moreover, when the flame appears at the pre-chamber nozzle, the pressure difference is already close to 0, indicating that the jet flame has no driving force and the pressure difference has no positive effect on the jet flame propagation. It suggests that the flame propagation in the main combustion chamber at this time is not caused by the flame jet from the pre-chamber, but by the free flame front propagation at the nozzle, and the main chamber fails to form an effective jet combustion. Meanwhile, the jet flame converges due to the weak jet strength and the turbulence disturbance inside the cylinder. The fuel in the main chamber is not ignited before the compression top dead center (TDC) due to the long flame propagation period in the pre-chamber. Consequently, the combustion in the main chamber starts only during the expansion stroke. Therefore, there is an increase in cylinder pressure at 20 °CA after the top dead center (ATDC), resulting in expansion work loss.

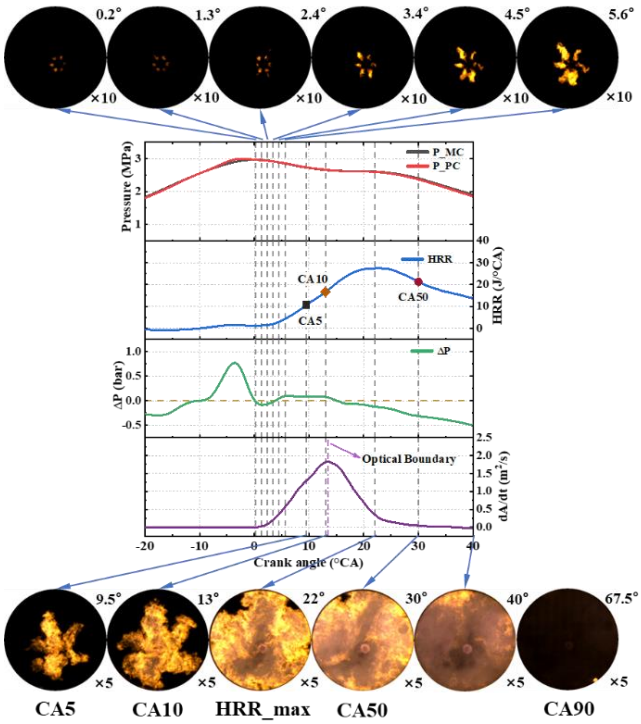

Fig. 3 The main chamber (MC) and pre-chamber (PC) pressures, main chamber heat release rate (HRR), pressure difference between MC and PC, flame area change rate (dA/dt), and jet flame development of a specific cycle under ammonia cracking ratios 0% and spark timing of 25° CA BTDC

When the ammonia cracking ratio is increased to 5% as illustrated in Figure 4, the MC and PC pressure and heat release rate (HRR) increase significantly. Compared with the pure ammonia combustion case, the peak pressure increases by 1 MPa, and the peak HRR by nearly 60%. Meanwhile, the combustion phase is significantly advanced, the flame propagation period in the pre-chamber is shortened by 6 °CA, and the CA50 is advanced by 16 °CA. The peak pressure difference increases to 1.38 bar, which brings a greater driving force for the flame propagation. Besides, the jet flame appears in MC at the moment corresponding to the peak pressure difference, indicating that the pressure difference positively affects the flame propagation in MC. It is conducive to accelerating the jet flame propagation speed in MC, and thus the peak flame area change rate is increased to 3.4 m^2/s. Although the combustion behavior under this condition has greatly improved compared to pure ammonia combustion, the jet intensity is still relatively low, and the upper left jet flame beam shows quenching in the middle of the flame at -3.4 °CA. In addition, the propagation direction of the jet flame still deviates due to the turbulence inside the cylinder.

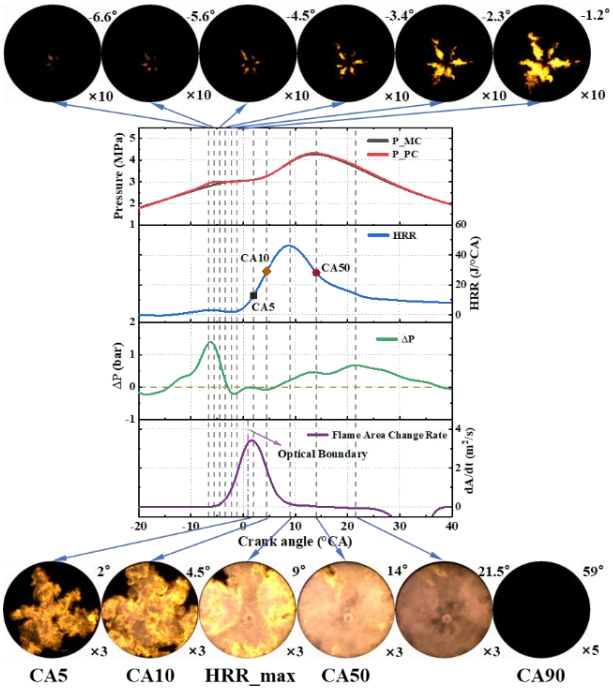

Fig. 4 The main chamber (MC) and pre-chamber (PC) pressures, main chamber heat release rate (HRR), pressure difference between MC and PC, flame area change rate (dA/dt), and jet flame development of a specific cycle under ammonia cracking ratio of 5%

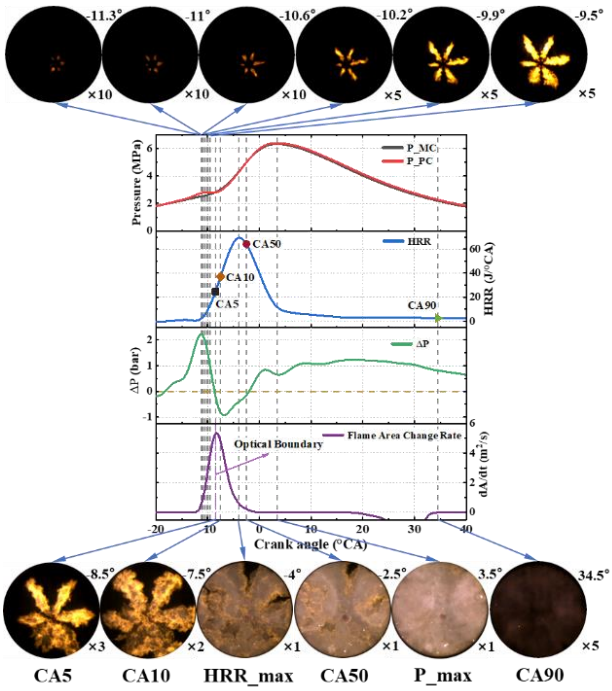

Fig. 5 The main chamber (MC) and pre-chamber (PC) pressures, main chamber heat release rate (HRR), pressure difference between MC and PC, flame area change rate (dA/dt), and jet flame development of a specific cycle under ammonia cracking ratio of 10%

When the ammonia decomposition ratio is increased to 10% as shown in Figure 5, the peak pressure rises to 6.33 MPa, the peak HRR to 69.3 J/(°CA), and the corresponding phase of the peak HRR is even advanced by 13 °CA. The pressure difference further increases to 2.2 bar, and the larger driving force brought by the increase in pressure difference makes the jet velocity faster, the jet intensity higher, and the jet flame shape more uniform and symmetrical. The peak flame area change rate increases to 5.3 m^2/s, significantly shortening the ignition delay and combustion duration. The combustion phase is further advanced, with CA50 occurring at -2.5 °CA. However, as CA50 occurs before the top dead center, most of the heat release takes place during the compression stroke, leading to negative work done by the combustion heat release. Therefore, it is necessary to investigate the impact of the spark timing (ST) on combustion performance under high ammonia cracking ratios and delay ST to ensure that the heat release peak occurs after the top dead center to further improve ammonia combustion performance.

3.2 Difference in combustion characteristics between PCI and SI mode

Figure 6 shows the changes in-cylinder pressure and heat release rate of pre-chamber ignition (PCI) and spark ignition (SI) under different ammonia cracking ratios. The experimental results show that with the increase of γ, the combustion performance in both combustion modes gradually improves. Under the pure ammonia combustion condition (i.e. γ=0%), the peak cylinder pressure and HRR of SI mode are higher than those of PCI mode. This is because the flame propagation distance is long and the heat transfer loss is severe in the PCI mode, which leads to combustion deterioration. Although multiple distributed ignition sites are generated, the weak jet intensity does not form effective jet combustion, and it is affected by turbulence to converge into flame clusters, resulting in its combustion performance being inferior to SI mode. Increasing γ to 2.5%, the ammonia combustion performance is improved in both ignition modes. However, the combustion performance of PCI is more significantly improved, with the peak heat release rate nearly doubling. Although the peak cylinder pressure in PCI mode is still lower than SI under this operating condition, the HRR of PCI mode is higher than that of SI. When γ increases to 5%, the combustion performance of PCI is significantly better than that of SI mode, with higher

cylinder pressure, more concentrated heat release, and more advanced phase corresponding to the peak HRR. When γ further increases to 10%, the peak cylinder pressure of PCI mode is as high as 6.23 MPa, which is 15% higher than that of SI (5.43 MPa), and the peak HRR is nearly 80% higher. The combustion performance is significantly better than SI. The distributed ignition of PCI mode greatly enhances the combustion speed of the fuel in MC and shortens the combustion duration. In general, ammonia cracking for hydrogen production has a greater improvement effect on the ammonia PCI mode than the SI mode, with a greater increase in HRR and a significant advance in the combustion phase.

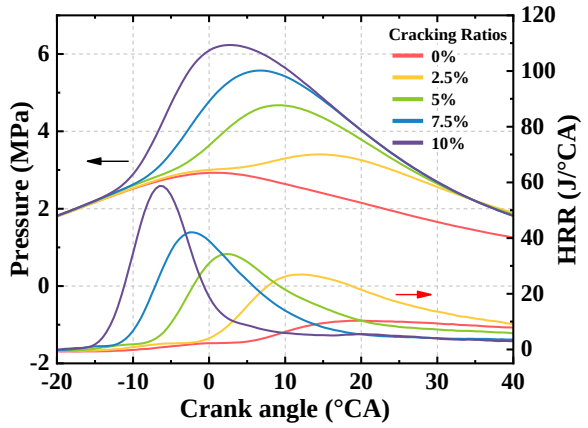

(a) PCI mode

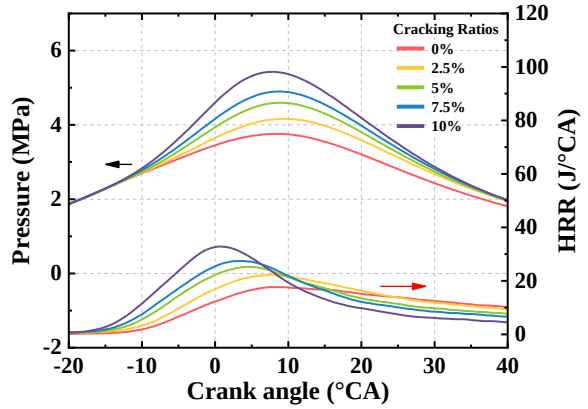

(b) SI mode

Fig. 6 Mean cylinder pressure and HRR of pre-chamber ignition (PCI) and spark ignition (SI) at different ammonia cracking ratios and spark timing of 25° CA BTDC

The difference in combustion phase between the pre-chamber ignition and spark ignition at different ammonia cracking ratios is illustrated in Figure 7. The results present that under pure ammonia conditions, the combustion phase is more advanced in SI mode, with a CA50 of 23.5 °CA, while CA50 is delayed by 9 °CA in PCI mode. Besides, the ignition delay period is shorter in SI mode, reduced by 6 °CA compared with PCI mode. This is due to the longer PC flame propagation time under pure ammonia combustion conditions in PCI mode. The combustion duration of the SI mode is longer than that of the PCI mode, which indicates that although the PCI mode is unable to form an effective jet combustion under pure ammonia conditions, the distributed ignition sites formed by the PCI mode can still accelerate the flame propagation speed in MC. With the increase of the ammonia cracking ratio, the ignition delay period and combustion duration of both ignition modes shorten. The change of ignition delay period and combustion duration is smaller in SI mode. However, the improvement of combustion performance is more significant in PCI mode, with a sharp reduction in ignition delay and combustion duration.

When γ increases from 0% to 5%, the ignition delay and combustion duration in SI mode are shortened by a total of 7.5 °CA, while in PCI mode by 12 °CA. When γ increases from 5% to 10%, the ignition delay and combustion duration in SI mode are shortened by 2.5 °CA, and in PCI mode by 12 °CA. The ignition delay of PCI mode is 10 °CA, and the combustion duration is 53.5 °CA at γ=10% case, which is shortened by 8.5 °CA and 6 °CA respectively compared to SI mode. In summary, under pure ammonia conditions, the longer PC flame propagation time, results in a significant heat transfer loss, and the combustion performance of PCI mode is worse than SI mode. As the ammonia cracking ratio increases, hydrogen addition more significantly improves the combustion performance of PCI mode. In PCI mode, the ignition delay and combustion duration are shortened significantly compared to SI mode, and the combustion phase is significantly advanced. Besides, as γ increases to a certain extent, the improvement effect of combustion performance in SI mode gradually weakens. When the decomposition ratio increases from 0% to 5%, the ignition delay and combustion duration are cumulatively shortened by 7.5 °CA. However, when the decomposition ratio further increases from 5% to 10%, the cumulative shortening of ignition delay and combustion duration is only 2.5 °CA.

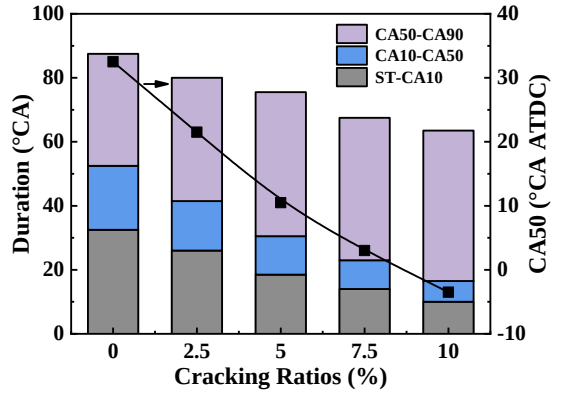

(a) PCI mode

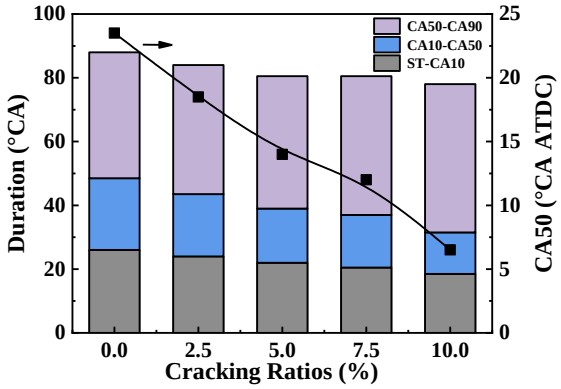

(b) SI mode

Fig. 7 The difference in combustion phase between the pre-chamber ignition and spark ignition at different ammonia cracking ratios

Figure 8 reveals the differences in indicated mean effective pressure (IMEP) and cycle-to-cycle variations of IMEP (COVIMEP) between pre-chamber ignition and spark ignition under different ammonia cracking ratios. It illustrates that the jet flame propagation speed in the main combustion chamber is low under pure ammonia conditions, due to the long PC flame propagation period and small pressure difference. This results in unstable combustion in PCI mode and extremely low IMEP. Though the combustion state is unstable with COV of 12% in SI mode, its stability is significantly better than that of PCI mode. As the ammonia cracking ratio increases, the IMEP of PCI mode substantially improves and the COV remarkably decreases. When the ammonia cracking ratio increases to 5%, the cycle variation decreased by 70%, indicating that the addition of hydrogen has a significantly positive effect on improving the combustion behavior of the PCI mode. When γ increases to more than 5%, the IMEP and COV of PCI mode gradually stabilize. As γ increases, the IMEP of SI mode continues to increase, and the COV keeps decreasing. However, the changes in the two parameters in SI mode are smaller compared to PCI mode. In addition, under the same γ, the combustion stability and IMEP of PCI mode are lower than those of SI mode, which is due to the significant heat transfer loss during the flame propagation process in the pre-chamber.

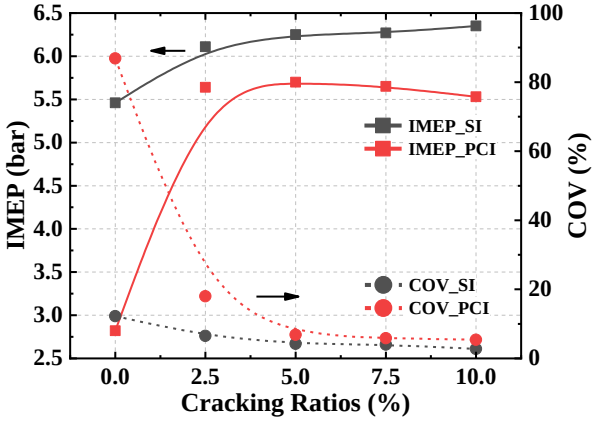

Fig. 8 IMEP and COVIMEP between the pre-chamber ignition and spark ignition at different ammonia cracking ratios

3.3 Comparison of jet flame development between PCI and SI mode

The natural flame luminosity (NFL) images of a specific single cycle are selected to analyze the flame development process in detail. The peak cylinder pressure of the selected single cycle is closest to the average pressure. Figure 9 displays the NFL images for both PCI and SI modes in a single cycle under different ammonia cracking ratios. The results illustrate that as the ammonia cracking ratio increases, the flame propagation speed significantly accelerates, the flame intensity enhances, and the combustion phase advances. Under low ammonia cracking ratio cases, the flame propagation speed is slow due to the low fuel activity, and the PC flame propagation time is longer, reaching up to 25 °CA under pure ammonia conditions. The flame propagation in MC is greatly affected by turbulence inside the cylinder. Six jet flames gradually converge at the nozzle to form a flame cluster, which continues to propagate in a flame shape similar to that of SI mode in the later stages of combustion. Increasing the ammonia cracking ratio, the combustion phase is gradually advanced, the intensity and speed of the jet flame increase significantly, and the 6 jet flames are more symmetrical and distinct. When the ammonia cracking ratio is increased to 5%, the higher jet intensity has significantly improved the jet flame speed. When the ammonia cracking ratio increases to 7.5%, the jet flame intensity further increases, with higher jet flame activity and faster propagation speed. The six jet flames propagate independently and rapidly, with the jet kinetic energy exceeding the effect of turbulent kinetic energy.

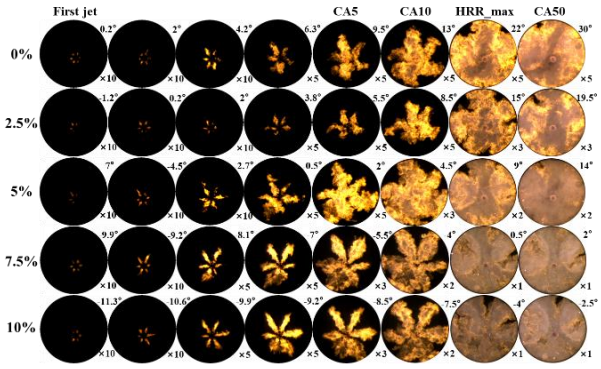

Fig. 9 The flame development of the pre-chamber ignition mode at different ammonia cracking ratios

Figure 10 presents that a flame kernel immediately forms around the spark plug after ignition and gradually propagates outward in the SI mode. Meanwhile, the charge temperature distribution significantly impacts on the ammonia flame propagation. Unlike methane, which spreads uniformly and symmetrically from the spark center to the surrounding areas, ammonia flame primarily propagates toward the direction of the exhaust valve (as shown in the upper right corner of the figure). As the ammonia cracking ratio increases, the flame propagation speed gradually accelerates, and the combustion phase advances. However, compared to the flame development images of the PCI mode shown in Figure 7 (a), the advancement of the combustion phase is smaller with the increase of γ. Taking γ increasing from 5% to 10% as an example, CA50 advances by 7 °CA in the SI mode, while in the PCI mode CA50 advances by 16.5 °CA in the PCI mode. In summary, the ignition delay in the PCI mode is longer under pure ammonia conditions due to the long PC flame propagation period. However, the flame combustion speed in the MC is faster in the PCI mode compared to the SI mode. As γ increases, the PCI mode gradually shows a more significant advantage in combustion speed.

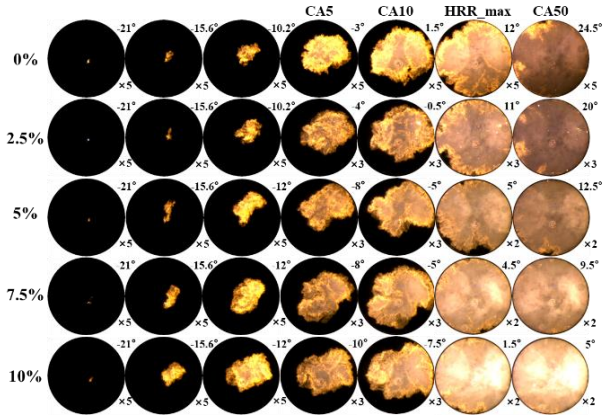

Fig. 10 The flame development of the spark ignition mode at different ammonia cracking ratios

Figure 11 illustrates the evolution of flame area for both ignition modes depicted in Figure 9 and Figure 10. The dashed line indicates the phase at which the jet flame front reaches the visualization boundary. The flame area changes have no practical significance after the dashed line and are only used as a reference for flame area comparison. The results show that the phase at which the flame area in the SI mode begins to increase significantly occurs earlier, which is due to the long PC flame propagation period in PCI mode. The flame area in the SI mode fills the visualization area of the combustion chamber earlier than in the PCI mode under pure ammonia combustion conditions. As the ammonia cracking ratio increases, the phase at which the flame covers the main chamber's visualization window gradually advances. Increasing γ from 0% to 10% results in a sharp increase in the flame area of the SI mode, while the increase in flame area is greater in the PCI mode. For the γ = 2.5% case, the effective flame propagation has not yet formed in the main chamber at 2 °CA ATDC in the PCI mode. Increasing γ to 5%, the flame covers 50% of the visualization area at 2 °CA ATDC. For γ = 2.5% case in the PCI mode, the flame fills the visualization window at 20°CA, while when γ increases to 10%, the phase advances by nearly 22 °CA. However, in the SI mode, when γ increases from 2.5% to 10%, the phase only advances by 12 °CA. It demonstrates that the reactivity improvement from ammonia cracking has a more significant impact on the combustion performance of the PCI mode.

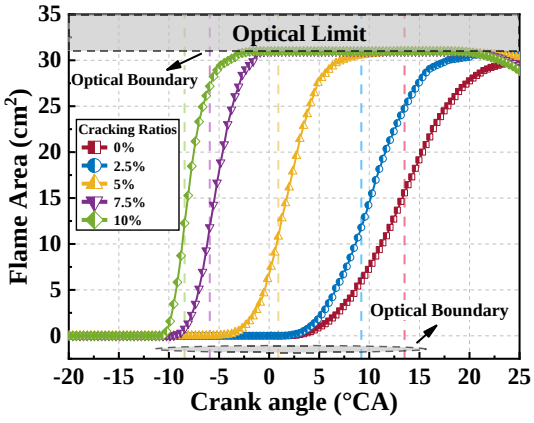

(a) PCI mode

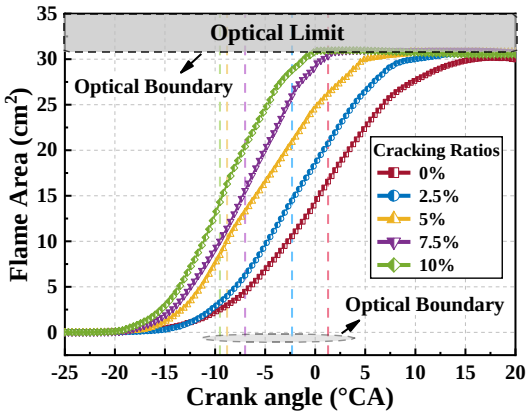

(b) SI mode

Fig. 11 The flame area in the pre-chamber ignition mode (a) and spark ignition mode (b) under different ammonia cracking ratios

The flame area change rate is used to characterize the combustion speed in MC. Figure 12 presents the flame area change rate for both ignition modes. Although the flame propagation phase in the PCI mode is later under the pure ammonia combustion condition, the MC peak flame propagation speed is higher than that of the SI mode due to the simultaneous diffusion and propagation of multiple flame kernels. This also explains why the ignition delay is longer while the combustion duration is shorter in the PCI mode under pure ammonia combustion conditions. As γ increases, the peak flame area change rate in the SI mode changes slightly. When γ increases from 0% to 10%, the peak flame area change rate in the SI mode increases by 0.63 m²/s, whereas it increases by 3.52 m²/s in the PCI mode. It demonstrates that due to the distributed ignition of the PCI mode, increasing fuel reactivity has a more significant impact on improving the ammonia flame propagation speed than the SI mode.

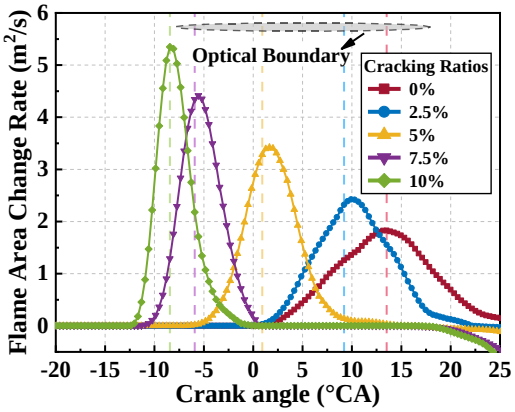

(a) PCI mode

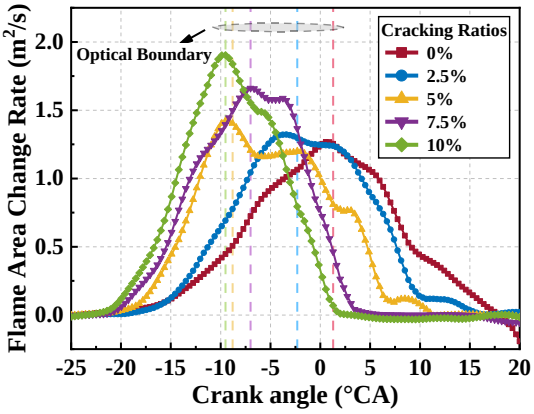

(b) SI mode

Fig. 12 The flame area change rate in the pre-chamber ignition mode (a) and spark ignition mode (b) under different ammonia cracking ratios

4 CONCLUSIONS

Ammonia combustion faces challenges of poor flammability and slow combustion. In this study, a passive pre-chamber with a narrow throat was designed, and natural flame luminosity (NFL) imaging was used to investigate the effects of hydrogen production by ammonia cracking on the combustion performance of pre-chamber ignition. The combustion behavior between the two ignition modes (PCI and SI) at different ammonia cracking ratios was compared. The main conclusions are as follows:

1) Increasing the ammonia cracking ratio (γ) from 0% to 10% effectively improves the combustion performance of the ammonia pre-chamber ignition. The fuel reactivity improvement increases the pressure buildup from 0.8 bar to 2.2 bar. The increase of pressure buildup accelerates the jet flame propagation speed, and shortens the ignition delay and combustion duration. When the ammonia cracking ratio increases to 7.5%, the jet flame propagation becomes more uniform and distinct.

2) Under pure ammonia combustion conditions, the combustion performance in the PCI mode is inferior to that of the SI mode. This is due to excessive heat transfer loss of the pre-chamber caused by the long PC flame propagation time, resulting in unstable combustion with a COV exceeding 80%.

3) As the ammonia cracking ratio increases, the combustion performance of ammonia in PCI mode significantly improves. In the SI mode, combustion performance gradually improves with increasing ammonia cracking ratio, but the improvement is relatively small. The peak flame area change rate in the SI mode increases by 0.63 m²/s, whereas it

increases by 3.52 m²/s in the PCI mode when increasing γ from 0% to 10%. It demonstrates that the reactivity improvement from ammonia cracking has more significant impact on PCI mode.

5 ACKNOWLEDGMENTS

This study was supported by the National Natural Science Foundation of China (Grant NO. 52206166, 52130605 and 51921004).

6 REFERENCES

[1] Qi Y, Liu W, Liu S, Wang W, Peng Y, Wang Z. A review on ammonia-hydrogen fueled internal combustion engines. eTransportation. 2023;18:100288.

[2] Kobayashi H, Hayakawa A, Somarathne KDKunkuma A, Okafor Ekenechukwu C. Science and technology of ammonia combustion. Proceedings of the Combustion Institute. 2019;37(1):109-33.

[3] Uddeen K, Tang Q, Shi H, Turner J. Performance and emission analysis of ammonia-ethanol and ammonia-methane dual-fuel combustion in a spark-ignition engine: An optical study. Fuel. 2024;358:130296.

[4] Nonavinakere Vinod K, Gore M, Liu H, Fang T. Experimental characterization of ammonia, methane, and gasoline fuel mixtures in small scale spark ignited engines. Applications in Energy and Combustion Science. 2023;16:100205.

[5] Liu S, Lin Z, Qi Y, Lu G, Wang B, Li L, et al. Combustion and emission characteristics of a gasoline/ammonia fueled SI engine and chemical kinetic analysis of NOx emissions. Fuel. 2024;367:131516.

[6] Ryu K, Zacharakis-Jutz GE, Kong S-C. Effects of gaseous ammonia direct injection on performance characteristics of a spark-ignition engine. Applied Energy. 2014;116:206-15.

[7] Lhuillier C, Brequigny P, Contino F, Rousselle C. Performance and Emissions of an Ammonia-Fueled SI Engine with Hydrogen Enrichment. SAE International; 2019.

[8] Lhuillier C, Brequigny P, Contino F, Mounaïm-Rousselle C. Experimental study on ammonia/hydrogen/air combustion in spark ignition engine conditions. Fuel. 2020;269:117448.

[9] Sun W, Zeng W, Guo L, Zhang H, Yan Y, Lin S, et al. An optical study of the combustion and flame development of ammonia-diesel dual-fuel engine based on flame chemiluminescence. Fuel. 2023;349:128507.

[10] Zhang S, Tang Q, Liu H, Yang R, Yao M. Numerical investigation and optimization of the ammonia/diesel dual fuel engine combustion under high ammonia substitution ratio. Journal of the Energy Institute. 2024;117:101797.

[11] Gross CW, Kong S-C. Performance characteristics of a compression-ignition engine using direct-injection ammonia–DME mixtures. Fuel. 2013;103:1069-79.

[12] Ryu K, Zacharakis-Jutz GE, Kong S-C. Performance characteristics of compression-ignition engine using high concentration of ammonia mixed with dimethyl ether. Applied Energy. 2014;113:488-99.

[13] Wen M, Liu H, Cui Y, Ming Z, Wang W, Wang X, et al. A study on optical diagnostics and numerical simulation of dual fuel combustion using ammonia and n-heptane. Energy. 2024;313:133977.

[14] Toulson E, Schock HJ, Attard WP. A Review of Pre-Chamber Initiated Jet Ignition Combustion Systems. SAE International; 2010.

[15] Liu Z, Zhou L, Wei H. Experimental investigation on the performance of pure ammonia engine based on reactivity controlled turbulent jet ignition. Fuel. 2023;335:127116.

[16] Bhandari R, Adhikari N. A comprehensive review on the role of hydrogen in renewable energy systems. International Journal of Hydrogen Energy. 2024;82:923-51.

[17] Klawitter M, Wüthrich S, Cartier P, Albrecht P, Herrmann K, Größnitzer C, et al. Ammonia as a fuel: Optical investigation of turbulent flame propagation of NH3/Air and NH3/H2/N2/Air flames at engine conditions. Fuel. 2024;375:132616.

[18] Liu J, Liu Z. In-cylinder thermochemical fuel reforming for high efficiency in ammonia spark-ignited engines through hydrogen generation from fuel-rich operations. International Journal of Hydrogen Energy. 2024;54:837-48.

[19] Zhou XY, Li T, Chen R, Wei YJ, Wang XR, Wang N, et al. Ammonia marine engine design for enhanced efficiency and reduced greenhouse gas emissions. NATURE COMMUNICATIONS. 2024;15(1).

[20] Liu W, Qi Y, Zhang R, Zhang Q, Wang Z. Hydrogen production from ammonia-rich combustion for fuel reforming under high temperature and high pressure conditions. Fuel. 2022;327:124830.

[21] Mercier A, Mounaïm-Rousselle C, Brequigny P, Bouriot J, Dumand C. Improvement of SI engine combustion with ammonia as fuel: Effect of ammonia dissociation prior to combustion. Fuel Communications. 2022;11:100058.

[22] Wang G, Tang H, Yang C, Magnotti G, Roberts WL, Guiberti TF. Quantitative laser-induced fluorescence of NO in ammonia-hydrogen-nitrogen turbulent jet flames at elevated pressure. Proceedings of the Combustion Institute. 2023;39(1):1465-74.

[23] Tang Q, Sampath R, Echeverri Marquez M, Hlaing P, Sharma P, Ben Houidi M, et al. Simultaneous Negative PLIF and OH* Chemiluminescence Imaging of the Gas Exchange and Flame Jet from a Narrow Throat Pre-Chamber. SAE International; 2020.

[24] Zhu S, Akehurst S, Lewis A, Yuan H. A review of the pre-chamber ignition system applied on future low-carbon spark ignition engines. Renewable and Sustainable Energy Reviews. 2022;154:111872.

[25] Alvarez CEC, Couto GE, Roso VR, Thiriet AB, Valle RM. A review of prechamber ignition systems as lean combustion technology for SI engines. Applied Thermal Engineering. 2018;128:107-20.

[26] Shah A, Tunestal P, Johansson B. Effect of Pre-Chamber Volume and Nozzle Diameter on Pre-Chamber Ignition in Heavy Duty Natural Gas Engines. SAE International; 2015.

[27] Gentz GR, Toulson E. Experimental Studies of a Liquid Propane Auxiliary Fueled Turbulent Jet Igniter in a Rapid Compression Machine. SAE International Journal of Engines. 2016;9(2):777-85.

[28] Gussak LA, Karpov VP, Tikhonov YV. The Application of Lag-Process in Prechamber Engines. SAE International; 1979.

[29] Hlaing P, Echeverri Marquez M, Bhavani Shankar VS, Cenker E, Ben Houidi M, Johansson B. A Study of Lean Burn Pre-Chamber Concept in a Heavy Duty Engine. SAE International; 2019.

[30] Echeverri Marquez M, Hlaing P, Tang Q, Sampath R, Ben Houidi M, Magnotti G, et al. High-Speed Imaging of Main-Chamber Combustion of a Narrow Throat Pre-Chamber under Lean Conditions. SAE International; 2020.

[31] Tang Q, Sampath R, Marquez ME, Sharma P, Hlaing P, Houidi MB, et al. Optical diagnostics on the pre-chamber jet and main chamber ignition in the active pre-chamber combustion (PCC). Combustion and Flame. 2021;228:218-35.

[32] Tang Q, Sampath R, Sharma P, Marquez ME, Cenker E, Magnotti G. Study on the effects of narrow-throat pre-chamber geometry on the pre-chamber jet velocity using dual formaldehyde PLIF imaging. Combustion and Flame. 2022;240:111987.

[33] Mei B, Zhang J, Shi X, Xi Z, Li Y. Enhancement of ammonia combustion with partial fuel cracking strategy: Laminar flame propagation and kinetic modeling investigation of NH3/H2/N2/air mixtures up to 10 atm. Combustion and Flame. 2021;231:111472.